analytical chemistry

pubs.acs.org/ac Letter

# Highly Selective Detection of $K^+$ Based on a Dimerized G-Quadruplex DNAzyme

Yu Cheng, Mingpan Cheng, Jingya Hao, Wenhui Miao, Wenqin Zhou, Guoqing Jia, and Can Li*

Cite This: *Anal. Chem.* 2021, 93, 6907−6912 Read Online

ACCESS | Metrics & More | Article Recommendations | Supporting Information

**ABSTRACT:** Potassium ion ($K^+$) plays a crucial role in biological systems, such as maintaining cellular processes and causing diseases. However, specifically, the detection of $K^+$ is extremely challenging because of the coexistence of the chemically similar ion of $Na^+$ under physiological conditions. In this work, a $K^+$ specific biosensor is constructed on the basis of a dimerized G-quadruplex (GQ) DNA, which is promoted by $K^+$, and the enzymatic activity of the resulting DNAzyme depends on the concentration of the $K^+$. The $K^+$ in a 1−200 mM concentration range can be selectively detected by visual color, UV−Vis absorbance or fluorescence even if the concentration of the accompanying $Na^+$ is up to 140 mM at an ambient condition up to 45 °C. In addition, this system can also be used to selectively detect $NH_4^+$ in a 5−200 mM concentration range. This dimerized DNAzyme offers a new type of biosensor with a potential application in the biological system.

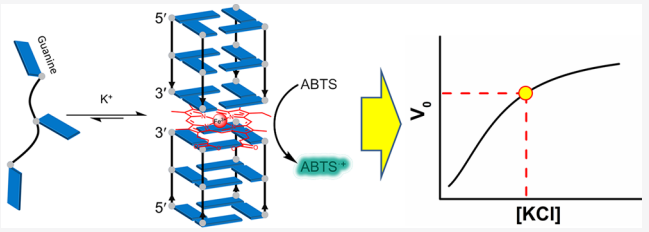




G-quadruplex (GQ) is a noncanonical nucleic acid structure with four helices formed by the guanine-rich sequence with several stacked G-quartets.[1] Cations, such as potassium ($K^+$), sodium ($Na^+$), or ammonium ($NH_4^+$) ions, are required for the GQ assembly.[2−5] These cations are sited in the channel of GQ and coordinated to the carbonyl oxygen atoms from guanines,[5,6] and the size and desolvation of cations determine the binding affinity of GQs.[7,8] Therefore, GQ is a type of natural biosensor for some specific cations.[9−14] Besides monomeric GQ, covalent dimeric GQ was also found to be used as a biosensor.[15,16]

$K^+$ is one of the most abundant cations in living cells and organisms, which is vital for cellular processes.[17] The intercellular and intracellular $K^+$ concentrations vary from around 10 to 140 mM in living organisms.[17] Abnormal $K^+$ homeostasis and dynamics are assumed to be related to diseases.[18] For example, the local $K^+$ levels within the tumor interstitial fluid are elevated to above 40 mM.[19] A number of GQ based $K^+$ sensors has been developed in the last two decades.[20−42] Though $K^+$-specific sensors constructed by fluorescent proteins[43,44] or small organic molecules[45−47] have been used under physiological conditions, the applications of these GQ based $K^+$ sensors are limited to physiological conditions because of either low sensing concentrations within a narrow detection range or a poor selectivity in the presence of a high concentration of $Na^+$.[20−42]

In this work, we developed a $K^+$ sensor based on the dimerized GQ, which is assembled from a $K^+$-supported GQ/hemin DNAzyme with a highly catalytic property.[48] Either visual color, UV−Vis absorbance or fluorescence can be an output. This dimerized DNAzyme is demonstrated to be a powerful sensor to specifically detect $K^+$ even in the presence of a high concentration of $Na^+$ or the presence of other kinds of metal ions (for example, $Li^+$, $Mg^{2+}$, $Ca^{2+}$, etc.) within a wide $K^+$ concentration range of 1−200 mM. The availability at temperatures up to 45 °C further demonstrates the feasibility for sensing *in vivo*. Besides being used as a $K^+$ sensor, this system is also available for $NH_4^+$ detection.

A six nucleotides sequence TTAG3 (5′-TTAGGG-3′) from human telomere folds into a stable GQ scaffold with three G-quartets as a monomer and further assembles into a dimer with six G-quartets through noncovalent stacking at the 3′ interface in the presence of $K^+$, as shown in Figure 1A, which has been characterized by NMR, nondenaturing polyacrylamide gel electrophoresis (PAGE), and size exclusion chromatography (SEC).[48−50] A peroxidase-mimicking DNAzyme could be formed by mixing the GQ DNA with hemin as a cofactor. Here, the oxidation of 2,2′-azino-bis(3-ethylbenzothiazoline-6-sulfonic acid) (ABTS) to a green product $ABTS^{\bullet+}$ by $H_2O_2$ was used to probe the activity of DNAzyme. The oxidative product $ABTS^{\bullet+}$ can be detected at the absorbance of 414 nm by UV−Vis measurement. It is found that there is an obvious absorbance change only in KCl, while in either LiCl or NaCl, the absorbance is at a background level (Figure 1B), indicative of a high selectivity toward $K^+$ over other alkali metal ions such as $Na^+$ and $Li^+$. PAGE analysis in Figure 1C shows that the

**Received:** February 25, 2021
**Accepted:** April 29, 2021
**Published:** April 30, 2021




https://doi.org/10.1021/acs.analchem.1c00872
*Anal. Chem.* 2021, 93, 6907−6912

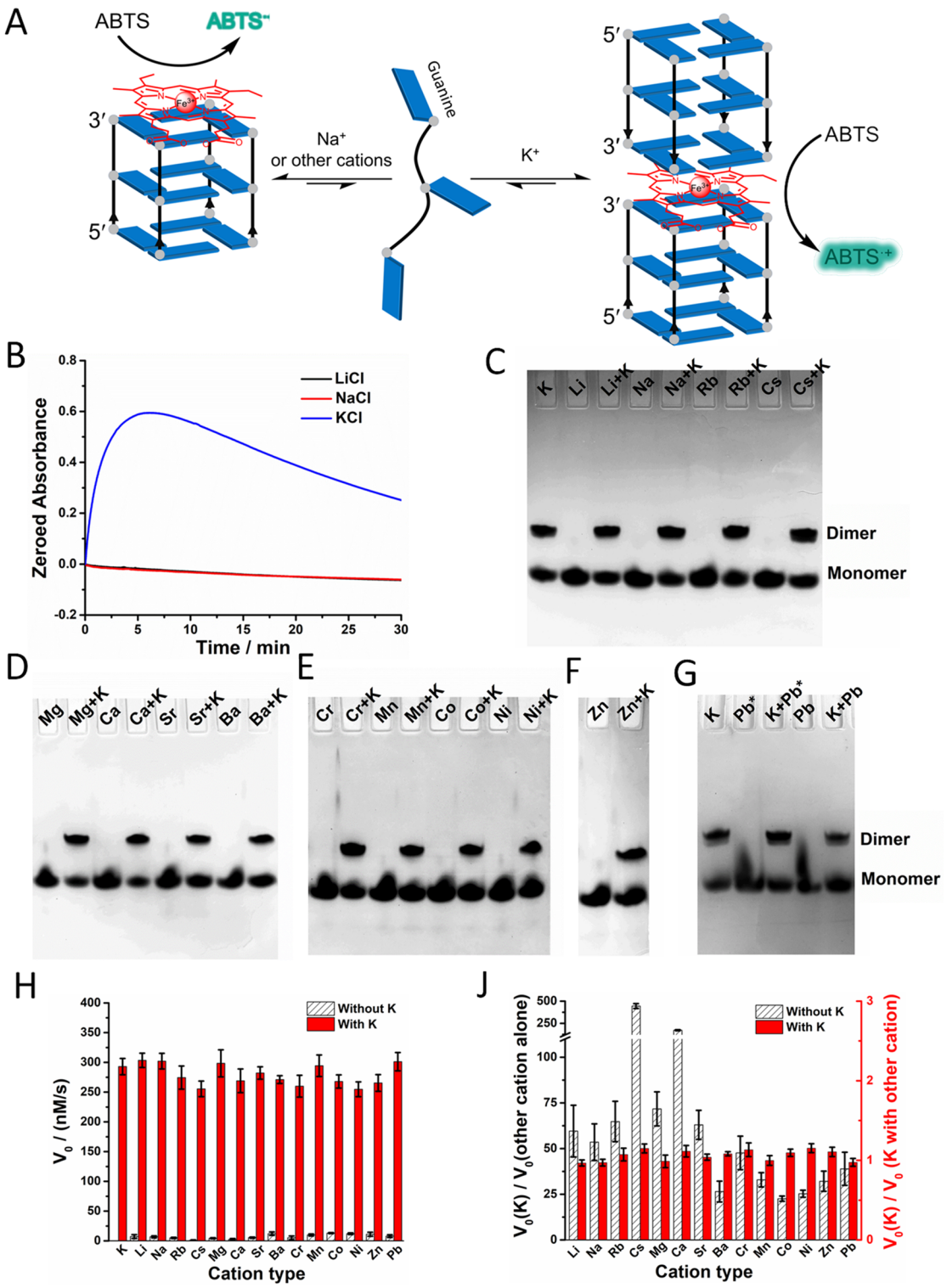


**Figure 1.** $K^+$ selectivity. (A) Schematic representation of the $K^+$-driven formation of the dimer GQ/hemin complex (right) and other cation-assisted folding of the monomer GQ/hemin complex (left). GQ and hemin are given in blue and red, respectively. Only three G-quartet layers of GQ are presented, and flanking residues are omitted. (B) Catalytic oxidation of ABTS (5 mM) promoted by $H_2O_2$ (1 mM) in the presence of GQ (1 $\mu$M) and hemin (0.1 $\mu$M) in 40 mM, pH 7.5 HEPES buffer with 100 mM LiCl, NaCl, or KCl and 0.05% (v/v) triton X-100 at 25 °C. The sample preparation procedure is optimized and summarized in Figure S2. PAGE analysis of TTAG3 in the presence of various other metal cations without or with 100 mM KCl (or $KNO_3$): (C) 100 mM LiCl, NaCl, RbCl, or CsCl; (D) 10 mM $MgCl_2$ or $CaCl_2$, 1 mM $SrCl_2$ or $BaCl_2$; (E) 100 $\mu$M $CrCl_3$, $MnCl_2$, $CoCl_2$, or $NiCl_2$; (F) 100 $\mu$M $ZnCl_2$; (G) 100 mM $KNO_3$, 10 $\mu$M(*), or 100 $\mu$M $Pb(NO_3)_2$. (H) Initial reaction velocity $V_0$ of TTAG3/hemin DNAzyme in different metal cations without and with 100 mM KCl. Reaction conditions and raw data are given in Figure S3. (J) Increasement folds of velocity $V_0$ of TTAG3/hemin DNAzyme in 100 mM KCl compared to other metal cations alone (black bar, left $Y$ axis) or in the presence of 100 mM KCl (red bar, right $Y$ axis).



https://doi.org/10.1021/acs.analchem.1c00872
Anal. Chem. 2021, 93, 6907−6912

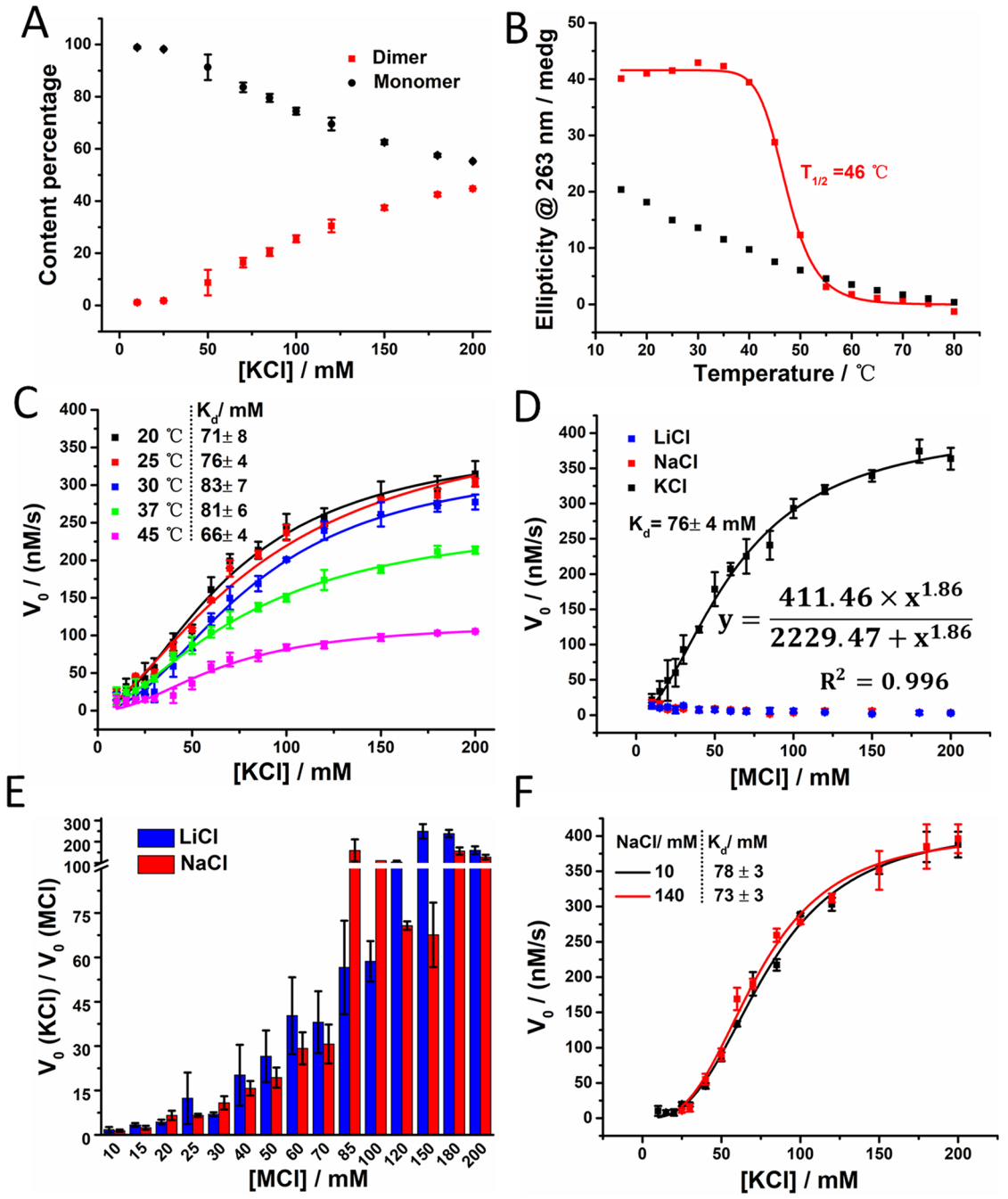


**Figure 2.** Dimer DNAzyme as a $K^+$ sensor. (A) SEC analysis of TTAG3 in 10 to 200 mM KCl. (B) CD melting profiles of TTAG3 at 260 nm in 25 mM KCl (black) and 140 mM KCl (red). (C) $V_0$ values of TTAG3/hemin DNAzymes at gradient temperatures and the calculated $K_d$ values. (D) $V_0$ of TTAG3/hemin DNAzyme in LiCl, NaCl, and KCl from 10 to 200 mM. (E) $K^+$ selectivity over $Li^+$ and $Na^+$: $V_0$ values of TTAG3/hemin DNAzyme in 10−200 mM ions of KCl, LiCl, or NaCl. (F) Catalytic activity of the TTAG3/hemin DNAzyme in 10−200 mM KCl in the presence of 10 mM NaCl (black) or 140 mM NaCl (red).

dimer GQ is formed in the presence of KCl without and with NaCl or LiCl, and only the monomer GQ is formed in the presence of LiCl or NaCl alone. PAGE of other common metal cations shows a similar result (Figure 1C−G). Circular dichroism (CD) spectra of TTAG3 shows the parallel structure of GQ formed in a high concentration of KCl is not disturbed by the coexistence of other metal cations (Figure S1A,B). Enzyme assay results in Figure 1H show only background activity in other mono-, di-, and trivalent metal cations, including $Rb^+$, $Cs^+$, $Mg^{2+}$, $Ca^{2+}$, $Sr^{2+}$, $Ba^{2+}$, $Cr^{3+}$, $Mn^{2+}$, $Co^{2+}$, $Ni^{2+}$, $Zn^{2+}$ and $Pb^{2+}$, but once KCl was added to the solution, the activity was restored to the same level of the condition containing KCl alone: the initial reaction $V_0$ after adding KCl to different metal cations increased from nearly zero to around 300 nM/s. These data of dimerized GQ DNAzyme in Figure 1J clearly show a high $K^+$ specificity and a strong anti-interference ability.

SEC is a powerful tool to distinguish the monomer from dimer GQs according to their difference in size.[48] SEC analysis results in Figure 2A show that the increasing concentration of


https://doi.org/10.1021/acs.analchem.1c00872
Anal. Chem. 2021, 93, 6907−6912

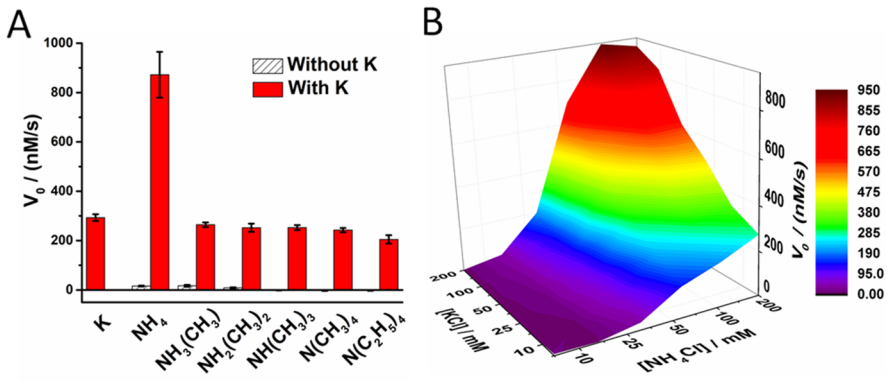


**Figure 3.** TTAG3/hemin DNAzyme as a $NH_4^+$ sensor. (A) Catalytic activity of the TTAG3/hemin DNAzyme in different ammonium cations without and with 100 mM KCl (raw data in Figure S10). (B) Calibration surface plot of $V_0$ as a function of $NH_4Cl$ and KCl concentration.

$K^+$ drives the GQ aggregation equilibrium from monomer to dimer. As we reported previously, the dimer species of GQ endues a much higher catalytic efficiency of GQ/hemin DNAzyme than that of the monomer fold.[48] The $V_0$ of TTAG3/hemin DNAzyme in gradient concentrations of KCl or $KNO_3$ was nearly the same, indicating that it is the $K^+$ cation but not the anion counterpart responsible for the activity, and $K^+$ sensing will not be affected by the anion counterpart (Figure S4). GQ is stabilized at a high concentration of $K^+$, and the melting temperature of GQ in 140 mM $K^+$ is 46 °C (Figures 2B and S5A,B). Then, the disassociation constants ($K_d$) for $K^+$ for this DNAzyme were measured under a temperature range of 20−45 °C. Figure 2C shows that there is a well fitted relationship between $V_0$ and the concentration of KCl, though the $V_0$ shows a limited decrease in the high temperature of 37 and 45 °C due to the partial dissociation of GQ (Figure 2B). $K_d$ values vary between 66 and 83 mM under 20−45 °C, which covers the physiological temperature range for a possible use *in vivo*.

The $V_0$ of TTAG3/hemin DNAzyme in different concentrations of LiCl, NaCl, or KCl was measured parallelly (Figure 2D). Low activity close to the background is observed in a wide concentration range of LiCl and NaCl up to 200 mM. Meanwhile, $V_0$ increases along with the increasement of KCl from 10 to 200 mM, leading to a $K^+$ disassociation constant ($K_d$) of 76 ± 4 mM with a detection limit of 5 mM estimated at the signal-to-noise ratio (S/N) of three. A high $K^+$ selectivity over $Na^+$ or $Li^+$ ($V_{0,KCl}/V_{0,NaCl\ or\ LiCl}$) is found in this large concentration range of 10−200 mM covering both intracellular and intercellular $K^+$ concentrations as shown in Figure 2E. $K^+$ selectivity even goes higher with the increasement of ion concentration and is up to more than 100 in the presence of 200 mM $Na^+$ or $Li^+$. In addition, the catalytic activity of DNAzyme can also be easily observed from the color change of the solution (Figure S6A,B): there was no color change in LiCl and NaCl, and as the concentration of KCl increased, the green color of the solution became deeper. Besides using UV−Vis absorbance and color change as outputs, the fluorescence was also investigated (Figure S7).[51] The $K^+$ concentration in goat serum detected by fluorescence also shows the potential applicability *in vivo*.

Figure 2F shows that presence of a low (10 mM, equivalent to the intracellular sodium concentration) or high (140 mM, equivalent to the intercellular sodium concentration) concentration of NaCl makes little difference in the catalytic activity of the TTAG3/hemin DNAzyme in the KCl range from 10 to 200 mM, which demonstrates the potential application of sensing $K^+$ *in vivo* again, especially considering the highly similar chemical properties between $K^+$ and $Na^+$. The TTAG3/hemin DNAzyme is different from all other GQ based $K^+$ sensors because its detection is based on the noncovalent dimerization of GQ,[52−58] and the exclusively high specificity to $K^+$ even in the presence of a high concentration of $Na^+$ is the most prominent advantage.

Besides metal cations, we further investigated the influence of ammonium cations on the DNAzyme activity. In the absence of $K^+$, $V_0$ values of TTAG3 in different types of ammonium salts are as low as the background (Figure 3A); in the presence of $K^+$, $NH_4^+$ can greatly enhance the enzymatic activity, whereas other types of ammoniums including methylammonium ($NH_3(CH_3)^+$), dimethylammonium ($NH_2(CH_3)_2^+$), trimethylammonium ($NH(CH_3)_3^+$), tetramethylammonium ($N(CH_3)_4^+$), and tetraethylammonium ($N(C_2H_5)_4^+$) exhibit no influence on the activities. This selectivity might be caused by the ability of $NH_4^+$ to coordinate to the iron center of hemin blocked by the larger size of the alkyl functional group in other types of ammonium salts.[59,60] PAGE shows that in ammonium alone TTAG3 remains as a monomer and the dimer occurs after the addition of KCl (Figures S7B and S8A). Then, $V_0$ values in gradient concentrations of $NH_4Cl$ were measured over 5−200 mM in the presence of different concentrations of KCl. The $V_0$ shows a linear relationship with the $NH_4Cl$ concentration at the given potassium concentrations (Figures 3B and S9). The calculated detection limit is 1.5 mM at S/N = 3 when the potassium concentration is 0, and the detection limit decreases as the potassium concentration increases (Figure S9). This shows the potential of the TTAG3/hemin DNAzyme to sense $NH_4^+$. The reaction activity also can be easily visualized by the color change of the solution (Figure S6C). PAGE analysis and melting temperatures of TTAG3 in 100 mM KCl and different concentrations of $NH_4Cl$ show that the existence of $NH_4Cl$ has little influence on the dimerization and thermal stability of GQ (Figures S5 and S8C).

The results of our TTAG3/hemin DNAzyme as a sensor for $K^+$ and $NH_4^+$ are summarized and compared with some reported results in Table S1. The TTAG3/hemin DNAzyme system can detect a wide range of $K^+$ concentrations of 1−200 mM with a high selectivity even in the presence of a high concentration of $Na^+$ and other metal cations. This DNAzyme system's availability for the dual detection of $K^+$ and $NH_4^+$ is a breakthrough in the area of sensing as the noncovalent


https://doi.org/10.1021/acs.analchem.1c00872
Anal. Chem. 2021, 93, 6907−6912

dimerization of the DNAzyme scaffold has never been applied as a biosensor.[52−58] The detection can be monitored by the visible light absorption measurement, fluorescence measurement or easily visualized by the color changes.

In this work, we developed a DNAzyme based $K^+$ sensor: $K^+$ drives the noncovalent dimerization of GQs, which boosts the activity of GQ based DNAzyme and triggers the color change to indicate the $K^+$ concentration. It was able to detect potassium concentrations over a large range from 1 to 200 mM at ambient temperatures of 20−45 °C with a high $K^+$ selectivity in the presence of a high concentration of $Na^+$ and a dozen of other metal cations. These results demonstrated that the dimer DNAzyme exhibits the possibility of sensing $K^+$ both intracellularly and intercellularly. In addition, this dimer GQ/hemin/$K^+$ DNAyzme is able to detect $NH_4^+$ in a concentration range from 5 to 200 mM with a high selectivity. This kind of sensing strategy of DNA scaffold dimerization may become a versatile strategy to further develop nucleic acid based biosensors.

## ■ ASSOCIATED CONTENT

### Supporting Information

The Supporting Information is available free of charge at https://pubs.acs.org/doi/10.1021/acs.analchem.1c00872.

Experimental methods, TTAG3/hemin as a dual sensor of the $K^+$ and $NH_4^+$ results, CD spectra, DNA sample preparation, ABTS oxidation, catalytic activity, CD melting profiles, photo of ABTS oxidation, and fluorescence measurements (PDF)

## ■ AUTHOR INFORMATION


### Corresponding Author

**Can Li** − *State Key Laboratory of Catalysis, Dalian Institute of Chemical Physics, Chinese Academy of Sciences, Dalian, Liaoning 116023, China;* orcid.org/0000-0002-9301-7850; Email: canli@dicp.ac.cn

### Authors

**Yu Cheng** − *State Key Laboratory of Catalysis, Dalian Institute of Chemical Physics, Chinese Academy of Sciences, Dalian, Liaoning 116023, China; University of Chinese Academy of Sciences, Beijing 100049, China*

**Mingpan Cheng** − *State Key Laboratory of Catalysis, Dalian Institute of Chemical Physics, Chinese Academy of Sciences, Dalian, Liaoning 116023, China;* orcid.org/0000-0003-1282-0076

**Jingya Hao** − *State Key Laboratory of Catalysis, Dalian Institute of Chemical Physics, Chinese Academy of Sciences, Dalian, Liaoning 116023, China; University of Chinese Academy of Sciences, Beijing 100049, China*

**Wenhui Miao** − *State Key Laboratory of Catalysis, Dalian Institute of Chemical Physics, Chinese Academy of Sciences, Dalian, Liaoning 116023, China; University of Chinese Academy of Sciences, Beijing 100049, China*

**Wenqin Zhou** − *State Key Laboratory of Catalysis, Dalian Institute of Chemical Physics, Chinese Academy of Sciences, Dalian, Liaoning 116023, China; University of Chinese Academy of Sciences, Beijing 100049, China*

**Guoqing Jia** − *State Key Laboratory of Catalysis, Dalian Institute of Chemical Physics, Chinese Academy of Sciences, Dalian, Liaoning 116023, China*

Complete contact information is available at: https://pubs.acs.org/10.1021/acs.analchem.1c00872


### Notes

The authors declare no competing financial interest.

## ■ ACKNOWLEDGMENTS

This work was supported by the National Key R&D Program of China (2017YFB0702800) and the Strategic Priority Research Program of the Chinese Academy of Sciences (Grant No. XDB17000000).

## ■ REFERENCES


(1) Bochman, M. L.; Paeschke, K.; Zakian, V. A. *Nat. Rev. Genet.* **2012**, *13*, 770−780.
(2) Sigel, A., Sigel, H., Sigel, R. K. O., Eds. *The alkali metal ions: their role for life*; Springer: Cham, Switzerland, 2016; pp 203−250.
(3) Largy, E.; Marchand, A.; Amrane, S.; Gabelica, V.; Mergny, J.-L. *J. Am. Chem. Soc.* **2016**, *138*, 2780−2792.
(4) Smargiasso, N.; Rosu, F.; Hsia, W.; Colson, P.; Baker, E. S.; Bowers, M. T.; Pauw, E. D.; Gabelica, V. *J. Am. Chem. Soc.* **2008**, *130*, 10208−10216.
(5) Ida, R.; Wu, G. *J. Am. Chem. Soc.* **2008**, *130*, 3590−3602.
(6) Wong, A.; Wu, G. *J. Am. Chem. Soc.* **2003**, *125*, 13895−13905.
(7) Zaccaria, F.; Fonseca Guerra, C. *Chem. - Eur. J.* **2018**, *24*, 16315−16322.
(8) Zaccaria, F.; Paragi, G.; Fonseca Guerra, C. *Phys. Chem. Chem. Phys.* **2016**, *18*, 20895−20904.
(9) Zhou, W.; Saran, R.; Liu, J. *Chem. Rev.* **2017**, *117*, 8272−8325.
(10) Liu, J.; Cao, Z.; Lu, Y. *Chem. Rev.* **2009**, *109*, 1948−1998.
(11) Mergny, J.-L.; Sen, D. *Chem. Rev.* **2019**, *119*, 6290−6325.
(12) Chen, J.; Zhang, Y.; Cheng, M.; Mergny, J.-L.; Lin, Q.; Zhou, J.; Ju, H. *Microchim. Acta* **2019**, *186*, 786−793.
(13) Hoang, M.; Huang, P.-J. J.; Liu, J. *ACS Sens* **2016**, *1*, 137−143.
(14) Yang, H.; Zhou, Y.; Liu, J. *TrAC, Trends Anal. Chem.* **2020**, *132*, 116060−116072.
(15) Jing, S.; Liu, Q.; Jin, Y.; Li, B. *Anal. Chem.* **2021**, *93*, 1333−1341.
(16) Ye, T.; Gao, H.; Zhang, Q.; Yan, C.; Yu, Y.; Fei, Y.; Gao, L.; Zhou, X.; Shao, Y. *Biosens. Bioelectron.* **2019**, *145*, 111703−111707.
(17) Thanzeel, F. Y.; Sripada, A.; Wolf, C. *J. Am. Chem. Soc.* **2019**, *141*, 16382−16387.
(18) Cheng, C. J.; Kuo, E.; Huang, C. L. *Semin. Nephrol.* **2013**, *33*, 237−247.
(19) Vodnala, S. K.; Eil, R.; Kishton, R. J.; Sukumar, M.; Yamamoto, T. N.; Ha, N. H.; Lee, P. H.; Shin, M.; Patel, S. J.; Yu, Z.; Palmer, D. C.; Kruhlak, M. J.; Liu, X.; Locasale, J. W.; Huang, J.; Roychoudhuri, R.; Finkel, T.; Klebanoff, C. A.; Restifo, N. P. *Science* **2019**, *363*, eaau0135.
(20) Ueyama, H.; Takagi, M.; Takenaka, S. *J. Am. Chem. Soc.* **2002**, *124*, 14286−14287.
(21) He, F.; Tang, Y.; Wang, S.; Li, Y.; Zhu, D. *J. Am. Chem. Soc.* **2005**, *127*, 12343−12346.
(22) Nagatoishi, S.; Nojima, T.; Juskowiak, B.; Takenaka, S. *Angew. Chem., Int. Ed.* **2005**, *44*, 5067−5070.
(23) Radi, A. E.; O'Sullivan, C. K. *Chem. Commun.* **2006**, 3432−3434.
(24) Wang, L.; Liu, X.; Hu, X.; Song, S.; Fan, C. *Chem. Commun.* **2006**, 3780−3782.
(25) Li, T.; Wang, E.; Dong, S. *Anal. Chem.* **2010**, *82*, 7576−7580.
(26) Sun, H.; Xiang, J.; Gai, W.; Liu, Y.; Guan, A.; Yang, Q.; Li, Q.; Shang, Q.; Su, H.; Tang, Y.; Xu, G. *Chem. Commun.* **2013**, *49*, 4510−4512.
(27) Liu, L.; Shao, Y.; Peng, J.; Huang, C.; Liu, H.; Zhang, L. *Anal. Chem.* **2014**, *86*, 1622−1631.
(28) Jarczewska, M.; Gorski, L.; Malinowska, E. *Sens. Actuators, B* **2016**, *226*, 37−43.
(29) Yang, L.; Qing, Z.; Liu, C.; Tang, Q.; Li, J.; Yang, S.; Zheng, J.; Yang, R.; Tan, W. *Anal. Chem.* **2016**, *88*, 9285−9292.

(30) Zhang, D.; Han, J.; Li, Y.; Fan, L.; Li, X. *J. Phys. Chem. B* **2016**, *120*, 6606−6611.
(31) Wu, T.; Ye, M.; Mao, T.; Lin, F.; Hu, Y.; Gan, N.; Shao, Y. *Anal. Chim. Acta* **2017**, *964*, 161−169.
(32) Deore, P. S.; Manderville, R. A. *Analyst* **2020**, *145*, 1288−1293.
(33) Lv, M.; Guo, Y.; Ren, J.; Wang, E. *Nucleic Acids Res.* **2019**, *47*, 9502−9510.
(34) Wu, Z. S.; Chen, C. R.; Shen, G. L.; Yu, R. Q. *Biomaterials* **2008**, *29*, 2689−2696.
(35) Yang, X.; Li, T.; Li, B.; Wang, E. *Analyst* **2010**, *135*, 71−75.
(36) Fan, X.; Li, H.; Zhao, J.; Lin, F.; Zhang, L.; Zhang, Y.; Yao, S. *Talanta* **2012**, *89*, 57−62.
(37) Lee, J.; Kim, H. J.; Kim, J. *J. Am. Chem. Soc.* **2008**, *130*, 5010−5011.
(38) Li, T.; Wang, E.; Dong, S. *Chem. Commun.* **2009**, *45*, 580−582.
(39) Li, T.; Wang, E.; Dong, S. *J. Am. Chem. Soc.* **2009**, *131*, 15082−15083.
(40) Wang, G.; Chen, L.; Zhu, Y.; He, X.; Xu, G.; Zhang, X. *Biosens. Bioelectron.* **2014**, *61*, 410−416.
(41) Chang, T.; Gong, H.; Ding, P.; Liu, X.; Cao, Z.; Shangguan, D.; et al. *Chem. - Eur. J.* **2016**, *22*, 4015−4021.
(42) Yang, Y.; Huang, J.; Yang, X.; Quan, K.; Xie, N.; Ou, M.; Tang, J.; Wang, K. *Chem. Commun.* **2016**, *52*, 11386−11389.
(43) Bischof, H.; Rehberg, M.; Stryeck, S.; Artinger, K.; Eroglu, E.; Waldeck-Weiermair, M.; Gottschalk, B.; Rost, R.; Deak, A. T.; Niedrist, T.; Vujic, N.; Lindermuth, H.; Prassl, R.; Pelzmann, B.; Groschner, K.; Kratky, D.; Eller, K.; Rosenkranz, A. R.; Madl, T.; Plesnila, N.; Graier, W. F.; Malli, R. *Nat. Commun.* **2017**, *8*, 1422−1433.
(44) Shen, Y.; Wu, S. Y.; Rancic, V.; Aggarwal, A.; Qian, Y.; Miyashita, S. I.; Ballanyi, K.; Campbell, R. E.; Dong, M. *Commun. Biol.* **2019**, *2*, 18−27.
(45) Liu, J.; Li, F.; Wang, Y.; Pan, L.; Lin, P.; Zhang, B.; Zheng, Y.; Xu, Y.; Liao, H.; Ko, G.; Fei, F.; Xu, C.; Du, Y.; Shin, K.; Kim, D.; Jang, S. S.; Chung, H. J.; Tian, H.; Wang, Q.; Guo, W.; Nam, J. M.; Chen, Z.; Hyeon, T.; Ling, D. *Nat. Nanotechnol.* **2020**, *15*, 321−330.
(46) Müller, B. J.; Borisov, S. M.; Klimant, I. *Adv. Funct. Mater.* **2016**, *26*, 7697−7707.
(47) Kong, X.; Su, F.; Zhang, L.; Yaron, J.; Lee, F.; Shi, Z.; Tian, Y.; Meldrum, D. R. *Angew. Chem., Int. Ed.* **2015**, *54*, 12053−12057.
(48) Cheng, Y.; Cheng, M.; Hao, J.; Jia, G.; Monchaud, D.; Li, C. *Chem. Sci.* **2020**, *11*, 8846−8853.
(49) Wang, Y.; Patel, D. J. *Biochemistry* **1992**, *31*, 8112−8119.
(50) Kato, Y.; Ohyama, K.; Mita, H.; Yamamoto, Y. *J. Am. Chem. Soc.* **2005**, *127*, 9980−9981.
(51) Golub, E.; Freeman, R.; Willner, I. *Anal. Chem.* **2013**, *85*, 12126−12133.
(52) Zhang, D.; Han, J.; Li, Y.; Fan, L.; Li, X. *J. Phys. Chem. B* **2016**, *120*, 6606−6611.
(53) Li, T.; Wang, E.; Dong, J. *Anal. Chem.* **2010**, *82*, 7576−7580.
(54) Sun, H.; Xiang, J.; Gai, W.; Shang, Q.; Li, Q.; Guan, A.; Yang, Q.; Liu, Y.; Tang, Y.; Xu, G. *Analyst* **2012**, *137*, 5713−5715.
(55) Dong, J.; Zhao, H.; Zhou, F.; Li, B. *Anal. Bioanal. Chem.* **2016**, *408*, 1863−1869.
(56) Chen, F.; Lu, Q.; Huang, L.; Liu, B.; Liu, M.; Zhang, Y.; Liu, J. *Angew. Chem., Int. Ed.* **2021**, *60*, 5453−5458.
(57) Wang, H.; Wang, D. M.; Gao, M. X.; Wang, J.; Huang, C. Z. *Anal. Methods* **2014**, *6*, 7415−7419.
(58) Sun, H.; Li, X.; Li, Y.; Fan, L.; Kraatz, H. B. *Analyst* **2013**, *138*, 856−862.
(59) Nakayama, S.; Sintim, H. O. *J. Am. Chem. Soc.* **2009**, *131*, 10320−10333.
(60) Gandolfi-Donadío, L.; Gallo-Rodriguez, C.; de Lederkremer, R. M. *Can. J. Chem.* **2006**, *84*, 486−491.


https://doi.org/10.1021/acs.analchem.1c00872
*Anal. Chem.* 2021, 93, 6907−6912